

# NMR Study of Large Skyrmions in $\text{Al}_{0.13}\text{Ga}_{0.87}\text{As}$ Quantum Wells

V. F. Mitrović<sup>1,2</sup>, M. Horvatić<sup>1</sup>, C. Berthier<sup>1</sup>, S. A. Lyon<sup>3</sup>, M. Shayegan<sup>3</sup>

<sup>1</sup> *Grenoble High Magnetic Field Laboratory, MPI-FKF and CNRS, B.P. 166, 38042 Grenoble Cedex 9, France*

<sup>2</sup> *Department of Physics, Brown University, Providence, RI 02912, U.S.A.*

<sup>3</sup> *Department of Electrical Engineering, Princeton University, Princeton, NJ 08544, U.S.A.*

(Dated: October 30, 2018)

A nuclear magnetic resonance (NMR) study is reported of multiple (30)  $\text{Al}_{0.13}\text{Ga}_{0.87}\text{As}$  quantum well (QW) sample near the Landau level filling factor  $\nu = 1$ . In these  $\text{Al}_{0.13}\text{Ga}_{0.87}\text{As}$  QWs the effective  $g$  factor is nearly zero. This can lead to two effects: vanishing electronic polarization ( $\mathcal{P}$ ) and skyrmionic excitations composed of a huge number of spins. As small  $\mathcal{P}$  values cause an overlap of the NMR signals from the QW and barriers, a special technique was employed to allow these two signals to be distinguished. The QW signal corresponds to a small, negative, and very broad distribution of spin polarization that exhibits thermally induced depolarization. Such a distribution can be attributed to sample inhomogeneities and/or to large skyrmions, the latter possibility being favored by observation of a very fast  $T_2^{-1}$  rate.

PACS numbers: 73.20.Mf, 73.21.Fg, 73.43.-f, 76.60.Lz

## I. INTRODUCTION

In two-dimensional electron systems (2DESs), the ground state at the Landau level filling factor  $\nu = 1$  is a ferromagnetic state where only the lowest Landau level is completely filled with spin-up electrons<sup>1</sup>. This spin-polarized state of a quantum Hall ferromagnet is particularly interesting because the low-lying charged excitations are skyrmions, complex charged spin texture<sup>2,3,4,5</sup>. The spin texture of a skyrmion encompasses many progressively reversed spins. Its size,  $S$ , is defined as the number of reversed spins within an elementary excitation. It is governed by the ratio,  $\eta \equiv E_Z/E_C$ , of the Zeeman energy,  $E_Z = g\mu_B H$ , limiting the number of spin flips, and the Coulomb interaction energy, favoring local ferromagnetic ordering<sup>5</sup>. Therefore, reducing  $E_Z$  towards zero leads to divergence of skyrmion size. One way to achieve this interesting limiting regime is to lower the effective  $g$  factor to nearly zero. This can be achieved either by the application of hydrostatic pressure, or as in the case of our sample by confining the 2DES to an  $\text{Al}_x\text{Ga}_{1-x}\text{As}$  quantum well (QW) where the Al composition ( $x$ ) is  $\simeq 0.13$ .

In pure GaAs QWs, where  $g \approx -0.44$ , a skyrmion size in the range  $3.6 < S < 9$  was inferred using different experimental techniques<sup>6,7,8,9,10,11</sup>. A large skyrmion size of  $S = 36$  was deduced from magnetotransport measurements under pressure<sup>12,13,14</sup>, in which the limit of  $g \rightarrow 0$  was reached. Although investigation of  $S$  using pressure seems to be very convenient for systematic exploration of the  $g$  dependence, it is compromised by two requirements: for each  $g$  (pressure) value, a separate cooldown is necessary and this leads to different disorder, and illumination of the sample is necessary to compensate for the loss of the density of 2DES induced by the application of pressure. An alternative possibility is to tune  $g$  to zero by confining the 2DES to  $\text{Al}_{0.13}\text{Ga}_{0.87}\text{As}$  QWs<sup>15,16</sup>. Using this approach, from their magnetotransport measurements in  $\text{Al}_{0.13}\text{Ga}_{0.87}\text{As}$  QW, Shukla *et al.*<sup>16</sup> reported the

largest ever skyrmions size  $S \approx 50$ .

Nuclear magnetic resonance (NMR) has proved to be a powerful tool for confirming the existence of skyrmionic excitations<sup>6</sup>. In addition, it has provided valuable information about the microscopic nature and dynamics of this many body electronic state<sup>6,17,18</sup>. Therefore, the NMR technique appears to be a good candidate for shedding light on the nature of the large skyrmions in  $\text{Al}_{0.13}\text{Ga}_{0.87}\text{As}$  QWs. Here, we present such an investigation.

We studied the <sup>71</sup>Ga NMR signal in a multiple  $\text{Al}_{0.13}\text{Ga}_{0.87}\text{As}$  QW sample, of the same composition as the one studied in Ref.<sup>16</sup>, at  $\nu = 1$ . The electronic polarization ( $\mathcal{P}$ ) is found to be very small, causing the overlap of signals from the QWs and barriers. The small  $\mathcal{P}$  would also inhibit the enhancement of the weak signal from QWs by optically pumped NMR, justifying our use of “conventional NMR”. A special technique was employed to distinguish between a weak signal from the QWs and one from the barriers. In these QWs we observe the thermally induced depolarization of small and negative (compared to a pure GaAs QW) spin polarizations. We argue that this can be attributed to large skyrmions.

The paper is organized as follows. In Sec. II experimental details are presented. These include descriptions of the sample, experimental setup, and essentials of NMR in QWs. The small tip angle technique is described in Sec. II C. Our findings are summarized in Sec. III. Finally, implications of these on the nature of elementary excitations are discussed in Sec. III C.

## II. EXPERIMENT

### A. Experimental Technique and the Sample

We investigated a multiple-QW sample, similar to the single QW sample used in transport measurements<sup>16</sup>. The results indicate that the sample is of high quality and

that its  $g$  factor is small<sup>16</sup>. Our sample consists of thirty 24 nm-wide  $\text{Al}_{0.13}\text{Ga}_{0.87}\text{As}$  QWs bounded on each side by 132 nm-thick  $\text{Al}_{0.35}\text{Ga}_{0.65}\text{As}$  ‘barriers’ which are Si doped near their centers. The density of the 2D electrons confined to each of the QWs is  $n_{2D} = 1.1 \times 10^{11} \text{ cm}^{-2}$  and their mobility is  $\mu_0 = 3 \times 10^4 \text{ cm}^2/\text{Vs}$ . The low mobility is believed to be predominantly due to impurity rather than alloy scattering<sup>16</sup>. The effective  $g$  factor for the 2D electrons in our sample is estimated to be  $g \approx +0.04$ <sup>16,19,20</sup>. It should be noted that this is of the opposite sign and an order of magnitude smaller than that in the bulk GaAs.

The NMR spectra were recorded using a custom built NMR spectrometer. For temperatures ( $T$ ) above 1 K we were not able to separate the QW signal due to insufficient signal-to-noise ( $S/N$ ) ratio in this sample. The low temperature environment, down to 50 mK, was provided by a  $^3\text{He}/^4\text{He}$  dilution refrigerator. The RF coil was mounted into the mixing chamber of the refrigerator. This ensured good thermal contact with the sample. We used the ‘bottom-tuning’ scheme in which a variable tuning capacitor was mounted as close as possible to the coil just outside of the mixing chamber. This tuning scheme minimizes the RF-losses, and so optimizes the NMR sensitivity. It allows a clear separation of the QW spectra at all temperatures below 1 K, otherwise impossible for  $T \gtrsim 200$  mK.

## B. NMR in Quantum Wells

In pure GaAs QW samples, previous optically pumped<sup>6</sup> and conventional NMR<sup>17</sup> studies have shown that NMR spectra consist of two well separated peaks originating from the nuclei located in the QWs and the barriers. These peaks are distinguishable owing to a significant polarization of the electrons in the QWs. This is because the hyperfine interaction between nuclei and electrons gives rise to the Knight shift,  $K_S$ , of the NMR line<sup>17,21,22</sup>

$$K_S(\mathbf{R}_i) \propto \mathcal{P}(\mathbf{R}_i)\rho_e(\mathbf{R}_i). \quad (1)$$

Here  $\mathcal{P}(R_i)$  is the local spin polarization at the spatial position,  $\mathbf{R}_i$ , of the nuclei, and  $\rho_e$  the local value of the electron density. Signal from nuclei in the barriers, where the electron density is vanishingly small, will be essentially unshifted, and can be used as a zero-shift reference. The nuclei in the QWs provide an NMR line whose shift is directly proportional to the average global electron polarization,

$$K_S(T) = A_c\rho_e(0)\mathcal{P}(T), \quad (2)$$

assuming uniform electronic density,  $\rho_e(0)$ . The effective hyperfine coupling constant,  $A_c$ , can be determined experimentally from the NMR shift obtained at low temperature, high field, and at filling factors, such as  $\nu = 1/3$ , where the 2DES is fully polarized, i.e.,  $\mathcal{P} = 1$  and  $K_S$

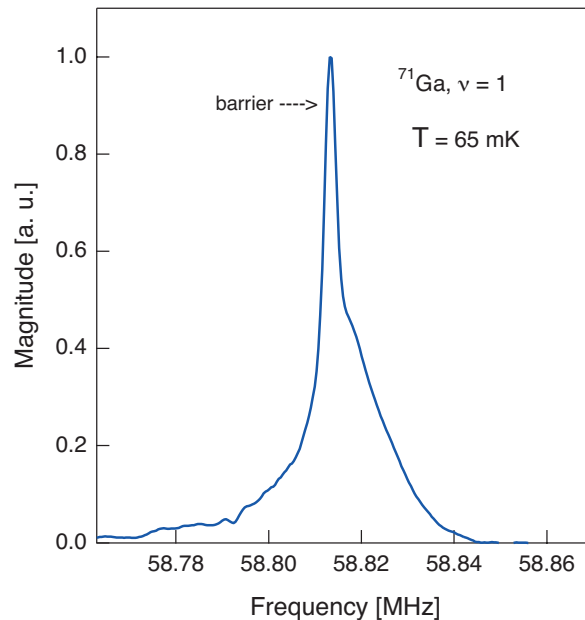


FIG. 1: (Color online) The  $^{71}\text{Ga}$  NMR spectrum, containing the signal from nuclei in both QWs and barriers, measured at  $\nu = 1$  and  $T = 65$  mK. The spectrum was recorded using the effective pulse length and the repetition times that favor the barriers’ signal (sharp narrow peak).

reaches its maximal value. From the values observed in pure GaAs multiple QW samples<sup>6,17</sup>, we infer that a maximum shift of  $K_S^{\mathcal{P}=1} \simeq 24$  kHz is expected for our sample. This allows for direct deduction of the spin polarization of 2DES from  $\mathcal{P} = K_S(T)/K_S^{\mathcal{P}=1}$ .

However, if the effective electronic  $g$  factor is lowered, the absolute polarization,  $|\mathcal{P}(g\mu_B H/k_B T)|$ , is smaller for the same value of  $H$  and  $T$ . As a consequence, the separation between the barrier and QW signals in NMR spectra is smaller as well. Indeed, as illustrated in Fig. 1, the NMR spectrum of the sample exhibits an asymmetric peak which contains contributions from the  $\text{Al}_{0.13}\text{Ga}_{0.87}\text{As}$  QWs (a broad, background-like signal) and from the barriers (a strong, narrow peak). Nevertheless, the two contributions can be discerned by exploiting their different nuclear spin-lattice relaxation times ( $T_1$ ). The hyperfine interaction responsible for the shift of the NMR line induces the  $T_1$  relaxation as well<sup>21</sup>. It contains spin operators of the form  $I_{\pm}S_{\pm}^e(\mathbf{R}_i)$  which produce simultaneous electronic,  $S^e$ , and nuclear spin,  $I$ , flips. In addition, the existence of closely spaced electron levels with energy separation comparable to the nuclear Zeeman gap is required by energy conservation. Such levels are provided by the additional degrees of freedom present in a real 2DES. These degrees of freedom could be generally ascribed to disorder and/or the presence of skyrmions in the electronic ground state in the vicinity of  $\nu = 1$ <sup>23,24,25,26,27</sup>. Therefore, even in the limit of vanishing  $g$  factor, we expect significantly faster  $T_1$  relaxation

of the nuclei in the QW compared to those in the barriers, due mostly to the existence of low energy excitations, such as skyrmions. This is further enhanced by the thermal depolarization.

The NMR spectra are recorded by the small tip angle free induction decay (FID) technique that we describe in detail in Sec. II C. The essence of this technique is that the signal intensity depends strongly on the effective pulse strength and the ratio of the repetition time between consecutive spectrum acquisitions and the relaxation time. Thus, one can find the tip angle that maximizes the  $S/N$  ratio, referred to as the *Ernst angle*<sup>28,29</sup> (Eq. 6 in the following sub-section). The two contributions to the NMR spectrum, having different relaxation rates, have different Ernst angles, as shown in Fig. 2. Therefore, we can obtain the pure QW spectrum from the analysis of the pulse strength dependence of the lineshape. The effective pulse strength, i.e. total pulse power, was varied in two ways: by varying the time of the pulse duration and by varying the voltage of the pulse, keeping its time duration fixed. The latter method is preferred since it eliminates the possible artifacts associated with the variable bandwidth coverage of the pulse.

We remark here that the small  $g$  factor also inhibits the application of the optical pumping technique. Thus, the only way to separate signal from nuclei in QWs and so probe the  $\mathcal{P}$  in these samples is by the conventional NMR, exploiting the different  $T_1$  relaxation times of nuclei in the QWs and barriers. The technique providing this “ $T_1$  contrast” is described in detail in the next sub-section.

### C. Small Tip Angle Pulse Technique

The small tip angle pulse method exploits the fact that the intensity of the NMR spectra depends strongly on the effective power (*i.e.*, the tip angle  $\theta$ ) of the excitation pulse and the ratio of the repetition time ( $T_R$ ) between consecutive spectrum acquisitions and the relaxation time ( $T_1$ ). In a conventional NMR experiment each data acquisition consists of an excitation and detection of magnetization, and usually enough time is allowed between acquisitions that the equilibrium spin temperature is fully restored,  $T_R \geq 5T_1$ . The spins are manipulated in several standard ways of which the two simplest examples are: FID ( $\frac{\pi}{2}$  – acquire) and Hahn echo ( $\frac{\pi}{2} - \tau - \pi$  – acquire) sequences. Usually, these sequences are repeated many times with a delay of  $T_R$  so that the signal is averaged in order to improve the signal-to-noise ratio.

As the echo sequence is rather incompatible with the small tip angles, in what follows we will only discuss the FID case used in our experiment. Following the exact  $\theta = \frac{\pi}{2}$  pulse the maximum signal intensity is obtained if  $T_R \geq 5T_1$ . In general, if the pulse angle is smaller and/or if one does not wait this long between consecutive acquisitions the signal will be smaller. However, one can show that the  $S/N$  ratio can be improved if short  $T_R$  are used

concomitantly with a smaller tip angle, *i.e.*, if  $\theta \lesssim \frac{\pi}{2}$ <sup>29</sup>. In this case the benefit in  $S/N$  from increasing the rate of data accumulation more than makes up for loss of signal from not allowing the magnetization to return to its thermal equilibrium value. Furthermore, the amplitude of the signal depends strongly on the spin-lattice relaxation rate. Therefore, tuning the excitation angle strength allows for separation of spectral components with distinct relaxation rates by optimizing respective signal amplitudes, as illustrated in Fig. 3. This is demonstrated in a more quantitative way in the next paragraph.

We consider the signal magnitude after consecutive data acquisitions. Following an excitation pulse, the longitudinal magnetization  $M_z$  of a system of spin 1/2 nuclei recovers towards its equilibrium value  $M_0$  by exponential relaxation,

$$M_z(t) = M_0 - (M_0 - M_z(t=0))e^{-t/T_1}, \quad (3)$$

where  $M_z(t=0)$  is the initial magnetization. After a time  $T_R$  the magnetization will recover to  $M = M_z(T_R)$ , prior to the next pulse which will rotate the magnetization by the angle  $\theta$  and restart the acquisition process. After this pulse the longitudinal magnetization will be equal to  $M \cos(\theta)$ , which is the starting magnetization of the following relaxation. Thus, in the steady state the above equation (at  $t = T_R$ ) becomes  $M = M_0 - (M_0 - M \cos(\theta))e^{-T_R/T_1}$ . Solving for  $M$ , one obtains

$$M = M_0 \frac{1 - e^{-T_R/T_1}}{1 - \cos(\theta)e^{-T_R/T_1}}. \quad (4)$$

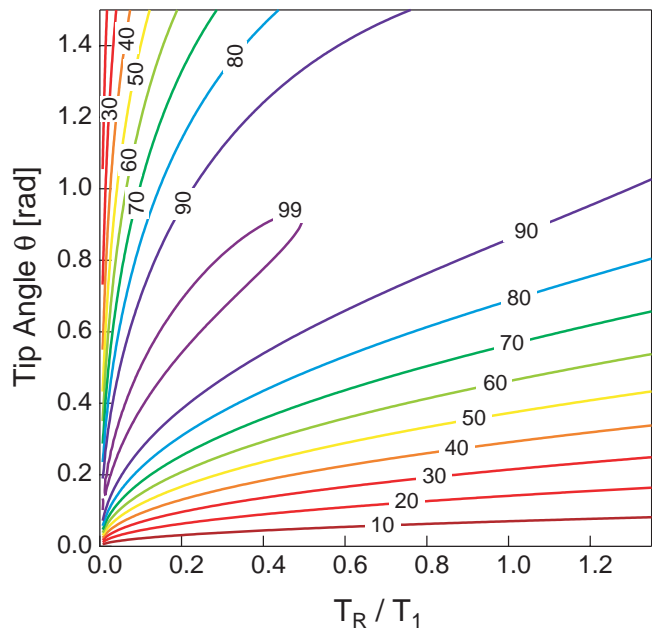


FIG. 2: (Color online) The contour-image plot of the signal-to-noise ratio as a function of an effective pulse tip angle and the ratio of the repetition time,  $T_R$ , to the spin-lattice relaxation time,  $T_1$ . The relative value of the  $S/N$  in percents is denoted on the contours.

In an experiment we detect a *transverse* magnetization just after the pulse, which is  $M \sin(\theta)$ . Thus, the signal magnitude is proportional to

$$S \propto \frac{1 - e^{-T_R/T_1}}{1 - \cos(\theta)e^{-T_R/T_1}} \sin(\theta).$$

The noise is inversely proportional to the square root of the number of averages  $N$ . Thus, in a given time it is proportional to  $\sqrt{T_R}$ . The signal to noise ratio is thus

$$S/N \propto \frac{(1 - e^{-T_R/T_1}) \sin(\theta)}{(1 - \cos(\theta)e^{-T_R/T_1}) \sqrt{T_R}}. \quad (5)$$

In Fig. 2 one can see that by concomitant shortening of the tip angle and the repetition time, one can maintain a high  $S/N$  ratio. From Eq. 5 it is easy to find that the tip angle that maximizes the  $S/N$  ratio is given by

$$\cos(\theta) = e^{-T_R/T_1}. \quad (6)$$

We remark that the detection of this angle allows one to determine  $T_1$  much faster than in the standard measurement. However, a  $T_1$  value determined in such a fashion certainly has higher error. In practice, in a non-homogeneous and complicated system such as QW samples this method of  $T_1$  determination turns out to be unsuitable.

### III. RESULTS AND DISCUSSION

#### A. Signal Separation

Full spectra at  $\nu = 1$  recorded using various effective pulse lengths at 65 mK are shown in Fig. 3. It is evident that the spectral shape is strongly dependent on the effective pulse angle, as previously discussed. Nonetheless, two main features can be discerned: a narrow Gaussian-like component at lower frequencies and a broad asymmetric component. The narrow component dominates the spectra obtained using weak excitation pulses. This implies that the signal comes from the nuclei with a very long relaxation time, *i.e.*,  $T_1 \rightarrow \infty$ , as suggested by Eq. 6 and Fig. 2. Indeed, signal from the nuclei in the barriers is expected to relax extremely slowly compared to the signal from QW. This is due to lack of free electrons in the barriers. Furthermore, the linewidth of this component is found to be 2 kHz, comparable to well separated barrier signals observed in other pure GaAs QW samples<sup>6</sup>. On the other hand, the broad asymmetric component dominates the spectra obtained using stronger excitation pulses, implying that this signal comes from the nuclei with relatively short relaxation times. This is expected for nuclei in QWs due to their hyperfine coupling with a significant number of free electrons. Therefore, the signal from the QWs can be obtained using stronger excitation pulses. This allows a separation of the two signals. The details of the procedure will be discussed next.

We first record the spectra using weak excitation pulses to obtain the precise spectral component from the barriers at a given temperature. The signal is fitted to a Gaussian that is then subtracted from the spectra recorded using strong excitation pulses. Spectra obtained in this manner contain only information from the nuclei in QWs, as illustrated in Fig. 4.

#### B. Electron Spin Polarization

After subtraction of the barriers' contribution from the NMR spectra we are left with a pure QW lineshape. Its temperature evolution is shown in Fig. 4. We point out that the spectral position defines the Knight shift,  $K_S(\nu = 1)$ , as discussed in Sec. II B. However, the most striking observation is the appearance of the significant linewidth broadening with decreasing temperature. The broadening is asymmetric. The notable width of the lower temperature spectra implies a significant distribution of the spin polarizations. Such a distribution can be attributed to sample inhomogeneities and/or to large skyrmions. We will address this issue in Sec. III C.

In addition to the linewidth broadening, decreasing temperature induces a shift of the average position of the QW signal. The temperature dependence of the linewidth and the lineposition are summarized in Fig. 5. We point out that the frequency scales of the figures can be directly related to the spin polarization, as the hyperfine coupling constant is known from measurements in pure GaAs QW samples. For our sample

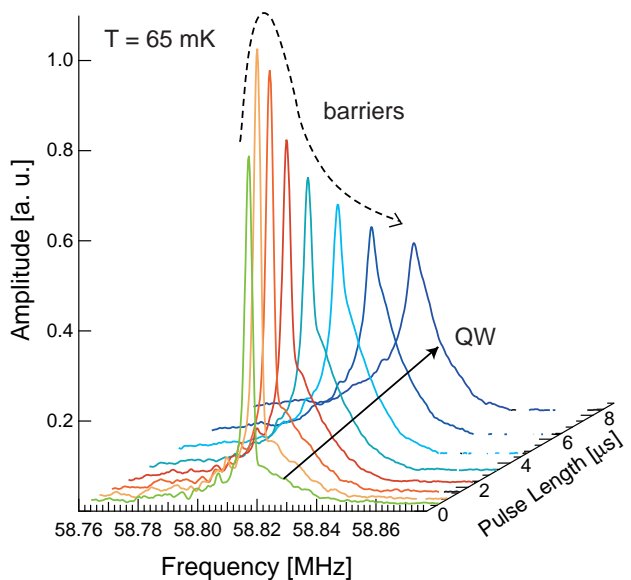


FIG. 3: (Color online) The  $^{71}\text{Ga}$  NMR spectra at  $\nu = 1$  taken by free induction decay. The effective pulse length dependence of the spectra is used to distinguish the signal of nuclei in QWs from the signal of those in barriers.

$K_S^{\mathcal{P}=1} = 24$  kHz corresponds to a full polarization, as discussed in Sec. II B. It is evident from Fig. 5 that the polarization is very small,  $\approx 1/8$  of the full polarization, and *negative* compared to pure GaAs QWs. This result is consistent with the small value of  $g \approx +0.04$  reported in Ref.<sup>16</sup> for a sample of the same Al concentration. One should note that this  $g$  value is much smaller in magnitude compared to  $g \simeq -0.44$  in pure GaAs QWs and has the opposite sign.

At the filling factor in the vicinity of but not at,  $\nu = 1$  the spin polarization is expected to be significantly smaller than at  $\nu = 1$  in the presence of large skyrmions<sup>6</sup>. We did not observe such a drop in polarization, possibly due to a small absolute value of the polarization at  $\nu = 1$ . Therefore, direct deduction of the skyrmion size was impossible. We remark that reduced spin polarization of the skyrmions at  $\nu = 1$  has already been reported even in pure GaAs multiple QW samples<sup>17</sup> presenting otherwise full polarization in the low- $T$  limit at  $\nu = 1/3, 1/2$  and  $2/3$ <sup>17,30</sup>. The full polarization  $\mathcal{P}(T \rightarrow 0, \nu = 1) = 1$  is approached only in very pure and homogeneous samples, preferably with smaller numbers of quantum wells<sup>6,18</sup>. The  $\text{Al}_{0.13}\text{Ga}_{0.87}\text{As}$  doped QWs are intrinsically less pure than pure GaAs ones. Thus, the observed reduction of  $\mathcal{P}(T \rightarrow 0, \nu = 1)$  is indeed much stronger and essentially no significant  $\nu$ -dependence of the shift and of the linewidth is observed in the range of  $\nu = 1 \pm 0.1$ . For this reason, a comparison of the  $\nu$  dependence with the one observed in Ref.<sup>18</sup> is inconclusive.

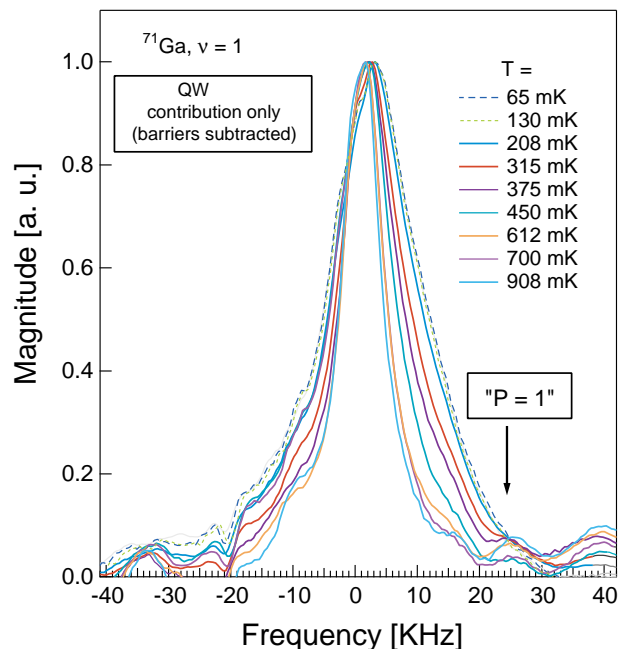


FIG. 4: (Color online) The temperature dependence of the QW signal. The zero of the frequency (i.e., the spin polarization) scale is defined by the position of the signal from barriers containing no free electrons. The position of the spectra defines the Knight shift,  $K_S(\nu = 1)$ .

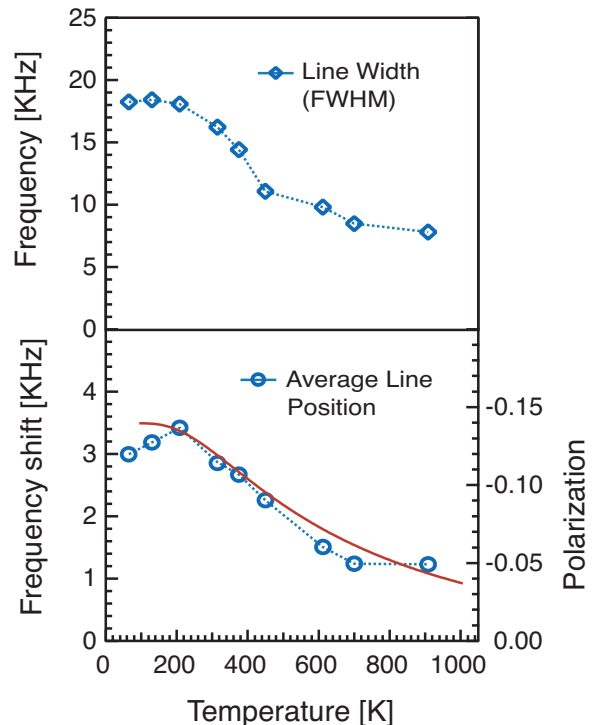


FIG. 5: (Color online) The temperature dependence (thermal depolarization) of the linewidth and lineposition (the shift,  $K_S$ ) of QW signal at  $\nu = 1$  shown in Fig.4. The dotted lines are guide to the eye. The solid line is the fit to tanh function as described in the text.

### C. Discussion

Since the temperature dependence of the shift probes low-lying excitations, a significant amount of theoretical work has been devoted to calculating the  $T$  dependence of the electron spin polarization precisely at  $\nu = 1$ <sup>31,32,33,34,35,36,37</sup>. In a simple model at  $\nu = 1$  for noninteracting 2D electrons with the chemical potential in the middle of the Zeeman gap,  $\mathcal{P}(T)$  is given by

$$\mathcal{P}(T, \nu = 1) = \tanh\left(\frac{E_Z}{4k_B T}\right). \quad (7)$$

In Fig. 5, we plot a fit to the above equation with  $E_Z$  as an adjustable parameter. Using the  $E_Z$  value obtained from the fit we find that  $g = 0.43 \pm 0.10$ . However, in pure GaAs QWs it was necessary to use a Zeeman splitting enhanced by a factor of  $\approx 10$  to fit the data<sup>6,38</sup>. This enhancement reveals the importance of interaction at  $\nu = 1$ . Assuming that the  $E_Z$  in our sample is enhanced by the same factor, we obtain  $g \approx 0.04$ , which is the same value as reported by Shukla *et al.*<sup>16</sup>. In other words, it appears that the nature of the interactions responsible for the gap enhancement at  $\nu = 1$  is similar in both GaAs and  $\text{Al}_{0.13}\text{Ga}_{0.87}\text{As}$  QWs.

Next, we will discuss the origin of the linewidth broadening at low temperatures. Two possible mechanisms

are sample inhomogeneities and/or large skyrmions. Dynamic measurements of the spin-spin decoherence time ( $T_2^{-1}$ ) are employed to differentiate between these. We have observed a very fast decay rate ( $T_2$ )<sup>-1</sup> of the amplitude of the spin echo (shorter than the dead time for signal detection,  $\sim 10 \mu\text{s}$ ), preventing us from pursuing more quantitative studies. Such dynamic fluctuations cannot be induced by the static sample inhomogeneities, since we were able to record spectra using free induction decay. Therefore, it is likely that our observations reveal some aspect of skyrmion physics. Mainly, a very fast ( $T_2$ )<sup>-1</sup> rate reveals that the spin polarization distribution presents strong dynamic fluctuations at the time scale of the spacing between the RF pulses (a few microseconds). These dynamic fluctuations can be associated with spintextured domains that are dynamic themselves and/or whose  $\nu$  distribution moves rapidly on the NMR time scale. We measured comparable  $\mathcal{P}$  and full width at half maximum (FWHM) values at  $\nu = 1$  and  $\nu = 1 \pm 0.1$ , which favors the dynamic  $\nu$  distribution scenario. Furthermore, in such a scenario,  $\mathcal{P}$  would be significantly diminished as is observed here and discussed in Ref.<sup>17</sup>. The most likely scenario is that dynamic variations of  $\nu$  are realized through skyrmion motion, meaning that they are concomitant with dynamic skyrmions.

This dynamic picture is endorsed by the temperature dependence of the linewidth (FWHM). Well-known NMR phenomena of motional narrowing implying that the FWHM is strongly affected by the dynamics of the nuclei<sup>21</sup>. Since the nuclei are spatially localized in the lattice, any observed dynamical effect must be related to the dynamics of electrons in QWs, i.e., to the motion of delocalized quasiparticles or skyrmions. The FWHM depicts an evolution of the skyrmion dynamics from the motionally-narrowed to the frozen regimes with decreasing temperature<sup>18</sup>. The slow skyrmion dynamics tend to increase the linewidth. However, the FWHM should ultimately decrease at very low  $T$  since the exponen-

tially small number of skyrmions cancels out the effect of the slow dynamics<sup>39</sup>. Therefore, the temperature dependence of the FWHM is expected to be nonmonotonic. As portrayed in Fig. 5, the FWHM continuously increases with decreasing temperature implying a progressive slowing down of skyrmion dynamics. Lack of the peak in the FWHM *versus*  $T$  graph indicates that skyrmions do not become fully localized<sup>39</sup> down to  $T = 65$  mK, the lowest  $T$  in our experiment. We remark further that the lack of the peak argues against the impurity scenario, since one expects impurities to be effective in pinning quasiparticles at such a low temperature.

#### IV. CONCLUSIONS

In a quantum wells sample with a small  $g$  tensor we have employed a special NMR technique to allow the distinction between a weak QW signal and the barrier signal. We determined the polarization of the electrons in the QWs and its temperature evolution. The measurements directly confirm the theoretical prediction ( $g \approx +0.04$ ) of a small, positive value for the  $g$  factor<sup>16</sup>. A very broad distribution of spin polarization was found in the sample. This can be attributed to sample inhomogeneities or to large skyrmions. The latter possibility is favored by observation of a very fast  $T_2^{-1}$  rate, indicating that the spin polarization distribution is dynamic rather than static.

We are grateful to Y. Tokunaga for useful discussions. Special thanks to P. van de Linden for technical assistance. This work was partially supported by the Grenoble High Magnetic Field Laboratory, under European Community contract RITA-CT-2003-505474, and by the NSF.

<sup>1</sup> S. M. Girvin, in *Topological Aspects of Low Dimensional Systems*, Proceedings of the Les Houches Summer School of Theoretical Physics, Session LXIX, 1998, edited by A. Comtet, T. Jolicœur, S. Ouvry, and F. David (Springer-Verlag and EDP Sciences, Berlin, (1999), p. 53.

<sup>2</sup> S. L. Sondhi, A. Karlhede, S. A. Kivelson, and E. H. Rezayi, Phys. Rev. B **47**, 16419 (1993); H. A. Fertig, L. Brey, R. Côté, and A. H. MacDonald, *ibid.* **50**, 11018 (1994).

<sup>3</sup> L. Brey, H. A. Fertig, R. Côté, and A. H. MacDonald, Phys. Rev. Lett. **75**, 2562 (1995).

<sup>4</sup> N. R. Cooper, Phys. Rev. B **55**, R1934 (1997); H. A. Fertig, L. Brey, R. Côté, A. H. MacDonald, A. Karlhede, and S. L. Sondhi, *ibid.* **55**, 10671 (1997).

<sup>5</sup> K. Lejnell, A. Karlhede, and S. L. Sondhi, Phys. Rev. B **59**, 10 183 (1999).

<sup>6</sup> S. E. Barrett, G. Dabbagh, L. N. Pfeiffer, K. W. West, and R. Tycko, Phys. Rev. Lett. **74**, 5112 (1995).

<sup>7</sup> A. Schmeller, J. P. Eisenstein, L. N. Pfeiffer, and K. W. West, Phys. Rev. Lett. **75**, 4290 (1995).

<sup>8</sup> E. H. Aifer, B. B. Goldberg, and D. A. Broido, Phys. Rev. Lett. **76**, 680 (1996).

<sup>9</sup> V. Bayot, E. Grivei, S. Melinte, M. B. Santos, and M. Shayegan, Phys. Rev. Lett. **76**, 4584 (1996).

<sup>10</sup> V. Bayot, E. Grivei, J.-M. Beuken, S. Melinte, and M. Shayegan, Phys. Rev. Lett. **79**, 1718 (1997).

<sup>11</sup> S. Melinte, E. Grivei, V. Bayot, and M. Shayegan, Phys. Rev. Lett. **82**, 2764 (1999).

<sup>12</sup> R. J. Nicholas, D. R. Leadley, D. K. Maude, J. C. Portal, J. J. Harris, and C. T. Foxon, J. Phys. C **10**, 11327 (1998).

<sup>13</sup> D. K. Maude, M. Potemski, J. C. Portal, M. Henini, L. Eaves, G. Hill, and M. A. Pate, Phys. Rev. Lett. **77**, 4604 (1996).

<sup>14</sup> D. R. Leadley, R. J. Nicholas, D. K. Maude, A. N. Utjuzh, J. C. Portal, J. J. Harris, and C. T. Foxon, Semicond. Sci. Technol. **13**, 671 (1998).

- <sup>15</sup> C. Weisbuch and C. Hermann, Phys. Rev. B **15**, 816 (1977).
- <sup>16</sup> S. P. Shukla, M. Shayegan, S. R. Parihar, S. A. Lyon, N. R. Cooper, and A. A. Kiselev, Phys. Rev. B **61**, 4469 (2000).
- <sup>17</sup> S. Melinte, N. Freytag, M. Horvatić, C. Berthier, L. P. Lévy, V. Bayot, and M. Shayegan, Phys. Rev. B **64**, 085327 (2001).
- <sup>18</sup> P. Khandelwal, A. E. Dementyev, N. N. Kuzma, S. E. Barrett, L. N. Pfeiffer, and K. W. West, Phys. Rev. Lett. **86**, 5353 (2001).
- <sup>19</sup> E. L. Ivchenko and A. A. Kiselev, Fiz. Tekh. Poprovodn. **26**, 1471 (1992) (Sov. Phys. Semicond. **26**, 827 (1992)).
- <sup>20</sup> A. A. Kiselev, E. L. Ivchenko, and U. Rössler, Phys. Rev. B **58**, 16 353 (1998).
- <sup>21</sup> A. Abragam *Principle of Nuclear Magnetism*. Oxford University Press, New York, (1961).
- <sup>22</sup> S. L. Richardson, M. L. Cohen, S. G. Louie, and J. R. Chelikowsky, Phys. Rev. B **33**, 1177 (1986).
- <sup>23</sup> I. D. Vagner and T. Maniv, Phys. Rev. Lett. **61**, 1400 (1988).
- <sup>24</sup> I.D. Vagner and T. Maniv, Physica B **204**, 141 (1995).
- <sup>25</sup> D. Antoniou and A. H. MacDonald, Phys. Rev. B **43**, 11686 (1991).
- <sup>26</sup> R. Côté, A. H. MacDonald, L. Brey, H. A. Fertig, S. M. Girvin, and H. T. C. Stoof, Phys. Rev. Lett. **78**, 4825 (1997).
- <sup>27</sup> A. G. Green, Phys. Rev. B **61**, R16 299 (2000).
- <sup>28</sup> B. Cowan. *Nuclear Magnetic Resonance and Relaxation*. Cambridge University Press, U. K., (1997).
- <sup>29</sup> R. R. Ernst and W. A. Anderson Rev. Sci. Instrum. **37**, 93 (1966).
- <sup>30</sup> S. Melinte, N. Freytag, M. Horvatić, C. Berthier, L. P. Lévy, V. Bayot and M. Shayegan, Phys. Rev. Lett. **84**, 354 (2000); N. Freytag, M. Horvatić, C. Berthier, M. Shayegan, L. P. Lévy, Phys. Rev. Lett. **89**, 246804 (2002); N. Freytag, Y. Tokunaga, M. Horvatić, C. Berthier, M. Shayegan, L. P. Lévy, Phys. Rev. Lett. **87**, 136801 (2001).
- <sup>31</sup> N. Read and S. Sachdev, Phys. Rev. Lett. **75**, 3509 (1995).
- <sup>32</sup> R. Haussmann, Phys. Rev. B **56**, 9684 (1997).
- <sup>33</sup> A.G. Green, Phys. Rev. B **57**, R9373 (1998).
- <sup>34</sup> J. P. Rodriguez, Europhys. Lett. **42**, 197 (1998).
- <sup>35</sup> T. Chakraborty and P. Pietiläinen, Phys. Rev. Lett. **83**, 5559 (1999).
- <sup>36</sup> M. Kasner, J. J. Palacios, and A. H. MacDonald, Phys. Rev. B **62**, 2640 (2000).
- <sup>37</sup> L. Brey, Phys. Rev. B **61**, 7257 (2000).
- <sup>38</sup> A. Usher, R. J. Nicholas, J. J. Harris, and C. T. Foxon, Phys. Rev. B **41**, 1129 (1990).
- <sup>39</sup> A. V. Ferrer, R. L. Doretto, and A. O. Caldeira, Phys. Rev. B **70**, 045319 (2004).